

# Increase in tropospheric nitrogen dioxide over China observed from space

Andreas Richter<sup>1</sup>, John P. Burrows<sup>1</sup>, Hendrik Nüß<sup>1</sup>, Claire Granier<sup>2,3,4</sup> & Ulrike Niemeier<sup>2</sup>

Emissions from fossil fuel combustion and biomass burning reduce local air quality and affect global tropospheric chemistry. Nitrogen oxides are emitted by all combustion processes and play a key part in the photochemically induced catalytic production of ozone, which results in summer smog and has increased levels of tropospheric ozone globally<sup>1</sup>. Release of nitrogen oxide also results in nitric acid deposition, and—at least locally—increases radiative forcing effects due to the absorption of downward propagating visible light<sup>2</sup>. Nitrogen oxide concentrations in many industrialized countries are expected to decrease<sup>3</sup>, but rapid economic development has the potential to increase significantly the emissions of nitrogen oxides<sup>4–7</sup> in parts of Asia. Here we present the tropospheric column amounts of nitrogen dioxide retrieved from two satellite instruments GOME<sup>8,9</sup> and SCIAMACHY<sup>10</sup> over the years 1996–2004. We find substantial reductions in nitrogen dioxide concentrations over some areas of Europe and the USA, but a highly significant increase of about 50 per cent—with an accelerating trend in annual growth rate—over the industrial areas of China, more than recent bottom-up inventories suggest<sup>6</sup>.

Measurements of the satellite instruments GOME and SCIAMACHY have been used to retrieve tropospheric columns of NO<sub>2</sub> from space<sup>8,11–13</sup>, and validation of the data product used in this study has been performed<sup>14</sup>. Analysis of the satellite data has revealed the spatial and temporal distribution of tropospheric NO<sub>2</sub> on a global scale (for example, see refs 8, 11–13, 15 and 16). These studies have highlighted the areas of intense pollution in industrialized regions, emissions from biomass burning, soil emissions and lightning signatures.

In contrast to *in situ* data from pollution monitoring networks, which measure the concentration near the ground, the remote sensing measurements, after correction for vertical sensitivity, yield the column amount integrated over the troposphere. With the exception of aircraft and lightning, the sources of nitrogen oxides (NO<sub>x</sub>) are located close to the surface. As a result of this NO<sub>x</sub> source distribution and the relatively short NO<sub>2</sub> chemical lifetime, the tropospheric NO<sub>2</sub> columns observed from space are dominated by the NO<sub>2</sub> amount in the boundary layer.

The NO<sub>2</sub> columns retrieved from space can be used to improve the currently uncertain estimates of NO<sub>x</sub> emissions. This requires knowledge of the lifetime of NO<sub>x</sub> and of the ratio NO<sub>2</sub>/NO<sub>x</sub> (refs 11, 17, 18). To a first-order approximation these values are independent of NO<sub>x</sub> concentrations<sup>17</sup>, and local changes in NO<sub>2</sub> columns can be assumed to be proportional to changes in local emission. The objective of this study has therefore been to investigate temporal changes in global tropospheric NO<sub>2</sub> patterns retrieved from GOME and SCIAMACHY measurements and thereby to infer changes in NO<sub>x</sub> emissions from 1996 to 2004. Initially, annual averages of tropospheric NO<sub>2</sub> columns derived from GOME measurements

were determined on a 0.5° × 0.5° grid for the years 1996–2002, during which the instrument provided global coverage. For each grid cell, a linear regression was performed. The resulting average gradients are shown in Fig. 1. For the majority of the globe the change in NO<sub>2</sub> amount over the period investigated is smaller than 6 × 10<sup>14</sup> molecules cm<sup>-2</sup> (~1 × 10<sup>14</sup> molecules cm<sup>-2</sup> yr<sup>-1</sup>), which is below the detection limit. However, significant reductions are observed over parts of Europe and the central east coast of the USA, in particular over the Ohio valley region, which has large power plants. At the same time, an increase in NO<sub>2</sub> is observed in the northeast of the USA as well as a large upward trend over parts of China.

To illustrate the extent and the spatial distribution of NO<sub>2</sub>, the averages of the tropospheric NO<sub>2</sub> columns derived using SCIAMACHY measurements from December 2003 to November 2004 are

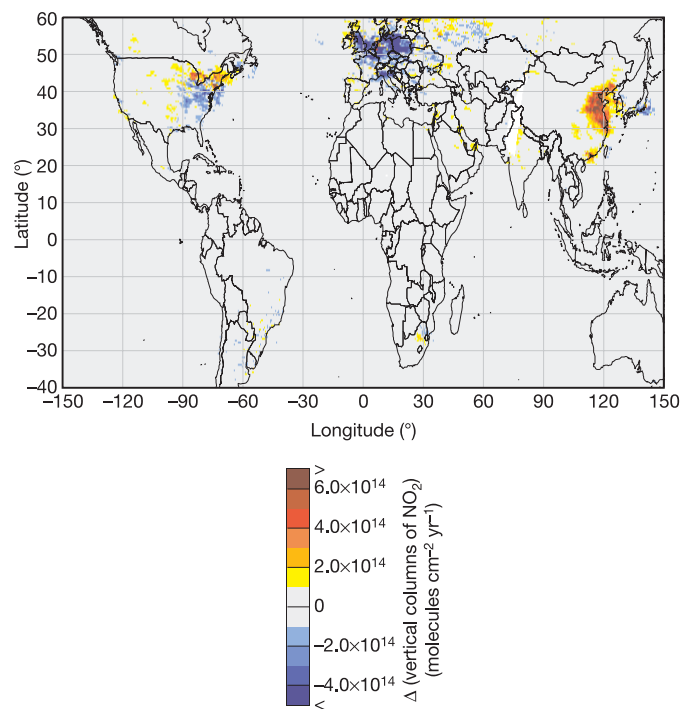


**Figure 1 | Average annual changes in tropospheric NO<sub>2</sub> as observed by GOME from 1996 to 2002.** The gradient obtained from a linear regression of the annual averages of tropospheric GOME NO<sub>2</sub> vertical columns, retrieved close to 10.30 a.m. LT from 1996 to 2002 is shown. Reductions in NO<sub>2</sub> are observed over Europe and the Central East Coast of the United States, while large increases are evident over China.

<sup>1</sup>Institute of Environmental Physics, University of Bremen, Otto-Hahn-Allee 1, D-28359 Bremen, Germany. <sup>2</sup>Max-Planck Institute for Meteorology, Bundesstraße 53, D-20146 Hamburg, Germany. <sup>3</sup>Service d'Aéronomie/IPSL, University of Paris 6, Paris 75005, France. <sup>4</sup>CIRES/NOAA Aeronomy Laboratory, 325 Broadway, Boulder, Colorado 80305, USA.

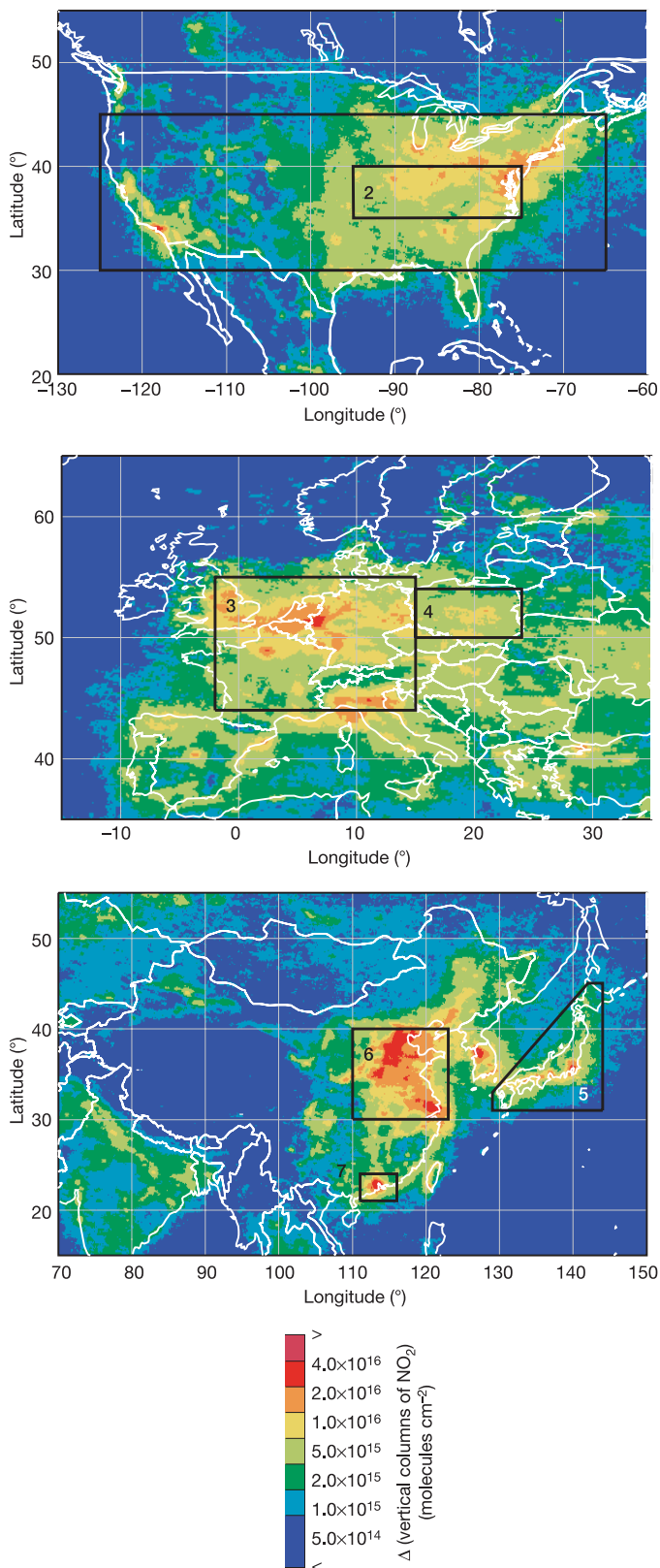


**Figure 2** | SCIAMACHY tropospheric  $\text{NO}_2$  vertical columns averaged between December 2003 and November 2004 for selected industrial regions. SCIAMACHY measurements are taken close to 10.00 a.m. LT. A nonlinear colour scale has been used because of the large range of  $\text{NO}_2$  vertical columns. The numbered rectangles indicate the regions used in Fig. 3.

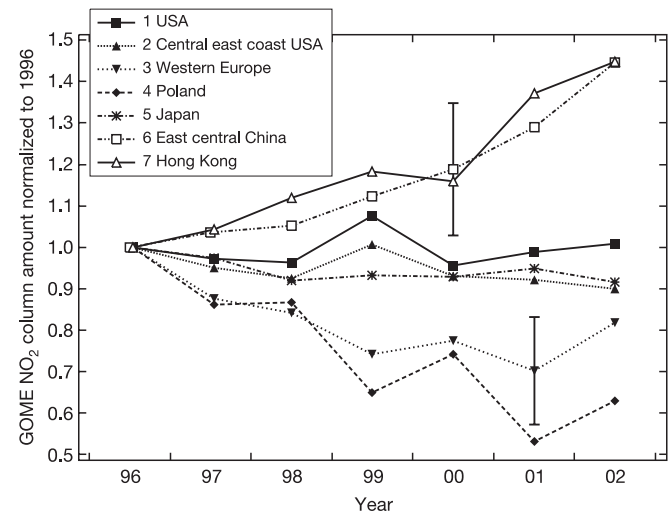


**Figure 3** | The temporal evolution of tropospheric  $\text{NO}_2$  columns from GOME for selected areas. The mean annual  $\text{NO}_2$  column amount normalized to that in 1996 for the geographical regions USA, Central East Coast USA, Western Europe, Poland, Japan, East Central China, and Hong Kong, which are defined in Fig. 2. The error bars represent the estimated uncertainty (s.d.) for an individual year, the values over China being larger as a result of the poorer knowledge and therefore larger uncertainty of the aerosol loading and its changes.

shown in Fig. 2 for North America, Europe and Asia. As expected, the largest changes are observed in areas with large  $\text{NO}_2$  columns. For the regions selected in Fig. 2, the temporal development of the  $\text{NO}_2$  column is shown in Fig. 3 relative to the value measured in 1996. It is evident from these time series that the changes depicted in Fig. 1 are systematic and not dominated by year-to-year variations, in particular over Europe and China. GOME retrieval errors have been discussed in detail in several publications<sup>12,17,19</sup>. Briefly, the error comprises an additive part, being approximately  $(0.5-1) \times 10^{15}$  molecules  $\text{cm}^{-2}$ , and a multiplicative part, being 40–60% for monthly averages over polluted regions. A large part of the error budget is associated with uncertainties in the assumptions made for the radiative transfer calculations, and is systematic, because the same air-mass factors are used for each year (see Methods). Consequently only changes in these parameters contribute to the relative error, shown in Fig. 3, and the uncertainty for an annual value is reduced to about 15%.

Reductions in  $\text{NO}_x$  emissions over the last two decades have been reported for some regions. For example, a 30%  $\text{NO}_x$  emission reduction for Europe between 1990 and 2000, and 18% from 1996 to 2002 has been published<sup>3</sup>, in excellent agreement with the GOME values shown in Fig. 3. These decreases are attributed to efforts to reduce emissions by the use of catalytic converters on automobile exhaust systems, the transition to cleaner fuels, changing economic circumstances, and so on.

The evolution of the columns of  $\text{NO}_2$  above the region of central east China ( $30^\circ\text{N}$ ,  $110^\circ\text{E}$  to  $40^\circ\text{N}$ ,  $123^\circ\text{E}$ ; see Fig. 2) are shown in more detail in Fig. 4, where monthly averages are plotted from both GOME and SCIAMACHY. A pronounced seasonal variation and a significant increase from year to year is observed, most notably in the winter values. The large  $\text{NO}_2$  annual cycle is explained by the seasonal variation of the lifetime of  $\text{NO}_x$  in the boundary layer<sup>16</sup>, related variations in meteorological conditions, and possibly also by higher winter emissions<sup>20</sup>.

The annual averages used for the linear regression in Fig. 1 are dominated by the winter values. However, if only summer months are analysed, a comparable increase of 42% (in May, June, July and August 1996–2002,  $\pm 20\%$ ) is found, indicating a consistent increase in  $\text{NO}_2$  concentrations over the industrialized part of China. This

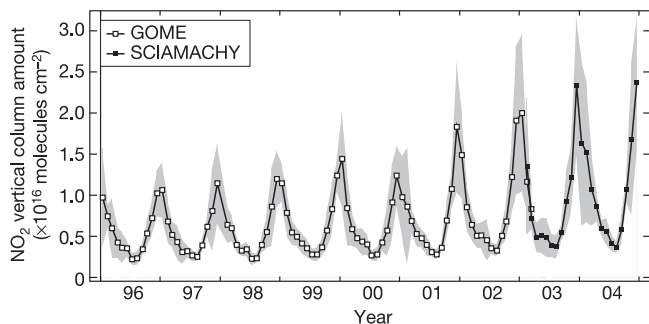


**Figure 4 | Monthly averages of tropospheric vertical columns of NO<sub>2</sub> over East Central China.** A plot of the monthly mean of the three-day composite of the tropospheric NO<sub>2</sub> vertical column versus time is presented for the area defined by latitudes 30° N to 40° N and longitudes 110° E to 123° E. Both GOME data (open symbols) and SCIAMACHY nadir measurements started in August 2002, but limited data are available prior to 2003. Shaded areas represent the standard deviation estimated for the monthly mean three-day composite, and take into account the variability of the measurements resulting from changes in NO<sub>2</sub> and data gaps arising from cloud cover and any missing observations.

growth accelerated over the past years, from a 4% annual increase in 1997 to 12% in 2002. These GOME results are supported by recent data from SCIAMACHY, also shown in Fig. 4. The two instruments made overlapping measurements from August 2002 to June 2003, and although the measurement pattern is not identical for the two instruments (see Methods), the resulting time series fit almost seamlessly together, indicating a continuing increase in NO<sub>2</sub> concentrations and ruling out unidentified drift or ageing issues in the GOME data record.

To interpret the observed behaviour of retrieved NO<sub>2</sub> and identify its origins, the following potential effects, which might explain an increase of the observed NO<sub>2</sub> columns over China, should be considered.

(1) Change in measurement sensitivity. The satellite sensitivity would increase if surface reflectance increased significantly. From the GOME data there is no indication for a systematic trend in reflectance. An increase in reflecting (sulphate) aerosols would also increase sensitivity, as would a reduction in black carbon and dust aerosols<sup>17</sup>. Aerosol precursor emissions of both black carbon and sulphate in China were reported to be lower in 2000 than in 1995 (ref. 6), while TOMS (total ozone monitoring spectrometer) ultraviolet absorbing aerosol optical depths show no trend over this period<sup>21</sup>. Given the lack of information on aerosol trends for China, we assume that the uncertainty introduced by aerosol changes from 1996 to 2002 is of the order of the 5–10% total effect of aerosols over the USA<sup>17</sup>.

(2) Change in NO<sub>2</sub>/NO<sub>x</sub> partitioning. Variation of the ratio of NO<sub>2</sub> to NO can lead to an apparent increase of NO<sub>2</sub> at constant NO<sub>x</sub>. The chemistry-transport model MOZART-2 (ref. 22) was used to quantify possible changes in the NO<sub>2</sub>/NO<sub>x</sub> ratio over Asia. A simulation was performed for the 1990–1999 period, where changes in surface emissions of all the chemical species included in MOZART were specified according to the POET emission scenario<sup>23</sup>. The results of the simulations showed that, for a 60% increase in emissions, typical of the increase in the anthropogenic emissions in China, the NO<sub>2</sub>/NO<sub>x</sub> ratio at the overpass time of GOME increased by 8% in summer and decreased by 3% in winter. These values are significantly lower than the NO<sub>2</sub> changes, retrieved from GOME and SCIAMACHY.

(3) Lifetime of NO<sub>2</sub>. This is determined primarily by the rate of production of HNO<sub>3</sub> from homogeneous and heterogeneous chemistry and its uptake in aerosol and clouds, and subsequent deposition. If OH concentrations are reduced, then for constant emissions, the observed NO<sub>2</sub> column increases. A decrease in OH

concentration can result from larger aerosol loading<sup>24</sup>, but on the other hand, increasing amounts of hydrocarbons from pollution are likely to increase OH levels. In any case an OH reduction would also have large effects on the lifetime of many other atmospheric trace gases. There is no evidence from measurements for a change in OH concentration sufficient to explain our observations of the changes in the retrieved tropospheric NO<sub>2</sub> columns.

(4) Increase in NO<sub>2</sub> emissions. As result of the rapidly growing economy powered by the generation of energy from fossil fuels, large increases have been predicted for NO<sub>x</sub> emissions from China<sup>4–7</sup>. The MOZART-2 model indicates that a 60% increase in anthropogenic NO<sub>x</sub> emissions results in a 50% increase of the NO<sub>2</sub> column in winter and 57% in summer over China. So to a first approximation, changes in NO<sub>2</sub> columns and changes in NO<sub>x</sub> emissions are expected to be of the same order of magnitude.

Thus, a significant increase in NO<sub>x</sub> emissions appears to be the most plausible explanation of the observed increase in NO<sub>2</sub> retrieved over China. In this context, a recent bottom-up inventory study<sup>6</sup> concluded that NO<sub>x</sub> emissions from China increased by 13% from 1994 to 2000, but showed signs of reducing growth rates between 1995 and 2000. Interestingly, this conclusion is not supported by GOME observations, which show a continuing increase in NO<sub>2</sub> columns. Apparently, any decreases in NO<sub>x</sub> emissions for example, from improved coal-fired power stations are more than offset by other changes in emissions or sources not yet included in the inventory. The number of vehicles has doubled from 10.4 million in 1995 to 20.5 million in 2002 in China<sup>25</sup>, and this in addition to increasing industrial and domestic heating sources could contribute to the observed increase of NO<sub>2</sub>. Detailed inventory studies are needed to confirm the conclusions drawn from the satellite observations and to assign emissions to sources. The rapid increases in NO<sub>2</sub> observed by GOME and SCIAMACHY over the last decade demonstrate that the expanding Chinese economy has significantly increased air pollution.

## METHODS

**GOME and SCIAMACHY.** GOME (Global Ozone Monitoring Experiment)<sup>8,9</sup> is a smaller version of SCIAMACHY (Scanning Imaging Absorption spectroMeter for Atmospheric CHartographY)<sup>10</sup>. Both are passive remote-sensing instruments observing the back-scattered radiance from the earth and the extraterrestrial irradiance. GOME measures in nadir whereas SCIAMACHY observes in alternate limb and nadir viewing.

The GOME is a four-channel ultraviolet/visible spectrometer observing scattered sunlight in nadir viewing geometry (ref. 8 and references therein). GOME is part of the core payload of the ESA ERS-2 platform, which was launched in April 1995 and provided global coverage from August 1995 to June 2003. The instrument observes simultaneously the spectral region from 240–793 nm having a channel-dependent spectral resolution of 0.2 to 0.4 nm. The ground scene of GOME typically has a footprint of 320 × 40 km<sup>2</sup>. With an across-track swath of 960 km, global coverage at the equator is achieved within three days.

SCIAMACHY was launched in March 2002 on ENVISAT. Nadir and limb data are available since August 2002. The ultraviolet/visible nadir measurements of SCIAMACHY used here are similar to those from GOME, the two main differences being the improved spatial resolution (60 × 30 km<sup>2</sup> over most parts of the world) at reduced coverage. The latter is a result of the alternate limb nadir viewing, global coverage at the Equator being achieved in six days.

**NO<sub>2</sub> data analysis.** Satellite data are analysed for tropospheric NO<sub>2</sub> in a four-step procedure. First, the NO<sub>2</sub> absorption averaged over all light paths contributing to the signal is determined using the Differential Optical Absorption (DOAS) method in the 425–450 nm region<sup>12</sup>. In the second step, the stratospheric component is removed by subtracting the daily stratospheric NO<sub>2</sub> column simulated by the 3d-CTM SLIMCAT<sup>26</sup> for the time of the satellite overpass. To account for differences between model and measurement, the SLIMCAT data are scaled to the GOME data over a clean region (180°–210° longitude). In a third step, a cloud screening is applied to remove those measurements with a cloud fraction of more than 0.2 as determined by the FRESCO algorithm<sup>27</sup>.

The last step is the conversion of the tropospheric residual to a vertical tropospheric column by accounting for the vertical sensitivity of the

measurement with the radiative transfer model SCIATRAN<sup>28</sup>. In this last step, a priori information is needed on surface spectral reflectance<sup>29</sup>, surface altitude, aerosol loading and the shape of the vertical distribution of NO<sub>2</sub>. The latter is taken from a run of the chemistry-transport MOZART-2 model (ref. 22) for 1997, which was used to determine monthly averaged air-mass factors on a 2.5° × 2.5° grid. Although the a priori assumptions used in the analysis have a significant impact on the retrieval results<sup>12,13,19</sup>, the observed changes in NO<sub>2</sub> are unlikely to be affected because the same input was used for all years (see Supplementary Information). Please note that for the year 1998, no GOME data are available for January. To avoid a bias in the annual averages from the seasonal variation in NO<sub>2</sub>, data from January 1997 were used instead.

Data analysis for GOME and SCIAMACHY is identical except that (1) SLIMCAT data are not yet available for 2004 and therefore the stratospheric correction is based on the use of a clean reference sector only, and (2) FRESCO cloud fractions are not yet available for all SCIAMACHY data and therefore an intensity criterion was used which was selected to be comparable to a threshold of 20% FRESCO cloud cover.

**MOZART model.** For the sensitivity studies, a MOZART-2 (ref. 22) model run at T63L47 (1.8–1.8° resolution) was used covering the time period 1990–1999. Emissions for all species for the 1990–1999 period are based on a linear interpolation for the years 1990–1995 and 1995–1997. The 1997 inventory has been compiled by combining the inventory for 1995 with regional trend data for various sources for 1995–1997. For the years 1997 to 1999 an extrapolation, based on the 1995–1997 trend, has been performed for each type of emission for each species<sup>23</sup>. These assumptions lead to a 60% increase in anthropogenic NO<sub>x</sub> emission over Central East China between 1990 and 1999.

Received 10 January; accepted 1 August 2005.

- Volz, A. & Kley, D. Evaluation of the Montsouris series of ozone measurements made in the nineteenth century. *Nature* **332**, 240–242 (1988).
- Solomon, S. *et al.* On the role of nitrogen dioxide in the absorption of solar radiation. *J. Geophys. Res.* **104** (D10), 12047–12058 (1999).
- Lövblad, G., Tarrasón, L., Tørseth, K. & Dutchak, S. (eds) *EMEP Assessment Part I. European Perspective The Cooperative Programme for Monitoring and Evaluation of the Long-range Transmission of Air Pollutants in Europe*, October 2004 48–51 (Norwegian Meteorological Institute, Oslo, 2004).
- van Aardenne, J. A., Carmichael, G. R., Levy, H. II, Streets, D. & Hordijk, L. Anthropogenic NO<sub>x</sub> emissions in Asia in the period 1990–2002. *Atmos. Environ.* **33**, 633–646 (1999).
- Streets, D. G. & Waldhoff, S. T. Present and future emissions of air pollutants in China: SO<sub>2</sub>, NO<sub>x</sub>, and CO. *Atmos. Environ.* **34**, 363–374 (2000).
- Streets, D. G. *et al.* An inventory of gaseous and primary aerosol emissions in Asia in the year 2000. *J. Geophys. Res.* **108** (D21), 8809, doi:10.1029/2002JD003093 (2003).
- Akimoto, H. Global air quality and pollution. *Science* **302**, 1716–1719 (2003).
- Burrows, J. P. *et al.* The Global Ozone Monitoring Experiment (GOME): Mission concept and first scientific results. *J. Atmos. Sci.* **56**, 151–175 (1999).
- European Space Agency, *GOME Global Ozone Measuring Experiment Users Manual* (ESA SP-1182, ESA/ESTEC, Noordwijk, 1995).
- Bovensmann, H. *et al.* SCIAMACHY—Mission objectives and measurement modes. *J. Atmos. Sci.* **56**, 127–150 (1999).
- Leue, C., Wenig, M., Wagner, T., Platt, U. & Jähne, B. Quantitative analysis of NO<sub>x</sub> emissions from GOME satellite image sequences. *J. Geophys. Res.* **106**, 5493–5505 (2001).
- Richter, A. & Burrows, J. P. Retrieval of tropospheric NO<sub>2</sub> from GOME measurements. *Adv. Space Res.* **29**, 1673–1683 (2002).
- Martin, R. V. *et al.* An improved retrieval of tropospheric nitrogen dioxide from GOME. *J. Geophys. Res.* **107**, 4437–4456 (2002).
- Petritoli, A. *et al.* First comparison between ground-based and satellite-borne measurements of tropospheric nitrogen dioxide in the Po basin. *J. Geophys. Res.* **109**, D15307, doi:10.1029/2004JD004547 (2004).
- Beirle, S., Platt, U., Wenig, M. & Wagner, T. Weekly cycle of NO<sub>2</sub> by GOME measurements: a signature of anthropogenic sources. *Atmos. Chem. Phys.* **3**, 2225–2232 (2003).
- Kunhikrishnan, T. *et al.* Analysis of tropospheric NO<sub>x</sub> over Asia using the model of atmospheric transport and chemistry (MATCH-MPIC) and GOME-satellite observations. *Atmos. Environ.* **38**, 581–596 (2004).
- Martin, R. V. *et al.* Global inventory of nitrogen oxide emissions constrained by space-based observations of NO<sub>2</sub> columns. *J. Geophys. Res.* **108**, 4537–4548 (2003).
- Richter, A. *et al.* Satellite measurements of NO<sub>2</sub> from international shipping emissions. *Geophys. Res. Lett.* **31**, doi:10.1029/2004GL020822 (2004).
- Boersma, K. F., Eskes, H. J. & Brinksma, E. J. Error analysis for tropospheric NO<sub>2</sub> retrieval from space. *J. Geophys. Res.* **109**, doi:10.1029/2003JD003962 (2004).
- Jaeglé, L., Steinberger, L., Martin, R. V. & Chance, K. Global partitioning of NO<sub>x</sub> sources using satellite observations: Relative roles of fossil fuel combustion, biomass burning and soil emissions. *Faraday Discuss.* **130**, 407–423, doi:10.1039/b502128f (2005).
- Massie, S. T., Torres, O. & Smith, S. J. Total Ozone Mapping Spectrometer (TOMS) observations of increases in Asian aerosol in winter from 1979 to 2000. *J. Geophys. Res.* **109**, D18211, doi:10.1029/2004JD004620 (2004).
- Horowitz, L. W. *et al.* A global simulation of tropospheric ozone and related tracers: description and evaluation of MOZART, version 2. *J. Geophys. Res.* **108** (D24), 4474, doi:10.1029/2002JD002853 (2003).
- Olivier, J. *et al.* Present and Future Surface Emissions of Atmospheric Compounds. POET (Precursors of Ozone and their Effects in the Troposphere) Report no. 2, 4–12 (EU project EVK2-1999-00011, 2003).
- Martin, R. V., Jacob, D. J., Yantosca, R. M., Chin, M. & Ginoux, P. Global and regional decreases in tropospheric oxidants from photochemical effects of aerosols. *J. Geophys. Res.* **108** (D3), 4097, doi:10.1029/2002JD002622 (2003).
- Zhao, J. & Gallagher, K. S. Clean vehicle development in China. *Sinosphere J.* **6**, 20, (<http://www.chinaenvironment.net/sino/sino14.pdf>) (2003).
- Chipperfield, M. P. Multiannual simulations with a three-dimensional chemical transport model. *J. Geophys. Res.* **104**, 1781–1805 (1999).
- Koelemeijer, R. B. A., Stammes, P., Hovenier, J. W. & de Haan, J. F. A fast method for retrieval of cloud parameters using oxygen A band measurements from the Global Ozone Monitoring Experiment. *J. Geophys. Res.* **106**, 3475–3490 (2001).
- Rozanov, V., Diebel, D., Spurr, R. J. D. & Burrows, J. P. GOMETRAN: a radiative transfer model for the satellite project GOME—the plane parallel version. *J. Geophys. Res.* **102**, 16683–16695 (1997).
- Koelemeijer, R. B. A., de Haan, J. F. & Stammes, P. A database of spectral surface reflectivity in the range 335–772 nm derived from 5.5 years of GOME observations. *J. Geophys. Res.* **108** (D2), 4070, doi:10.1029/2002JD002429 (2003).

**Supplementary Information** is linked to the online version of the paper at [www.nature.com/nature](http://www.nature.com/nature).

**Acknowledgements** GOME and SCIAMACHY I<sub>v0</sub> and I<sub>v1</sub> spectra were provided by ESA through DFD/DLR. We thank M. Chipperfield for providing SLIMCAT data. This study has been funded in part by the research programmes of the University of Bremen, the Max Planck Society, the European Union, German Aerospace (DLR), the German Ministry of Science and Education (BMBF) and the European Space Agency (ESA).

**Author Information** Reprints and permissions information is available at [npg.nature.com/reprintsandpermissions](http://npg.nature.com/reprintsandpermissions). The authors declare no competing financial interests. Correspondence and requests for materials should be addressed to A.R. ([richter@iup.physik.uni-bremen.de](mailto:richter@iup.physik.uni-bremen.de)).